International Journal of Modern Physics A
Vol. 24, No. 5 (2009) 1057–1067

World Scientific
www.worldscientific.com

EFFECTS OF THE WIGGLER ON THE HEFEI LIGHT SOURCE STORAGE RING

HE ZHANG* and MARTIN BERZ†

Department of Physics and Astronomy, Michigan State University, East Lansing, MI, 48824, USA
**zhanghe@msu.edu*
†berz@msu.edu

The Hefei light source (HLS) is a second generation synchrotron radiation light source, in which a superconducting wiggler is installed and operating. The effects of the wiggler on the beam dynamics on the HLS storage ring are studied, in order to make sure the wiggler can operate properly when the ring is working in the high brilliance mode. We generate a model of the magnetic field in the midplane of the wiggler. The 3D magnetic field model is also builded up by COSY infinity 9.0. Both the linear and nonlinear effects of the wiggler are discussed. The vertical tune is changed from 2.535 to 2.567 and the vertical beta function is heavily distorted, while a symplectic tracking study shows the dynamic aperture is only slightly affected by the wiggler. And the wiggler should be able to run on the high brilliance mode after the linear effects get compensated.

Keywords: Wiggler; nonlinear effects; differential algebra.

1. Introduction

The Hefei light source (HLS) is a second generation dedicated VUV radiation light source. It is composed of a 200 MeV linac and an 800 MeV storage ring. The storage ring consists of four triple bend achromat (TBA) cells and four 3 m long straight sections. The characteristic wavelength of the bending radiation is 2.4 nm. In order to meet the requirement of the hard X-ray synchrotron radiation users, a superconducting wiggler was installed on the storage ring. The characteristic wavelength of the wiggler radiation is 0.485 nm, and its usable wavelength is extended to 0.097 nm, which lies in the hard X-ray range.[1]

HLS runs in general purpose light source (GPLS) operation mode now. The emittance in this mode is 133 nm · rad. A high brilliance light source (HBLS) operation mode was proposed, in which the emittance was reduced to 27 nm · rad. The tunes of HBLS are (5.2073, 2.5351). The β functions and dispersion function of HBLS are shown in Fig. 1. In the following, we are going to discuss the effects of the wiggler when the storage ring runs in HBLS mode.

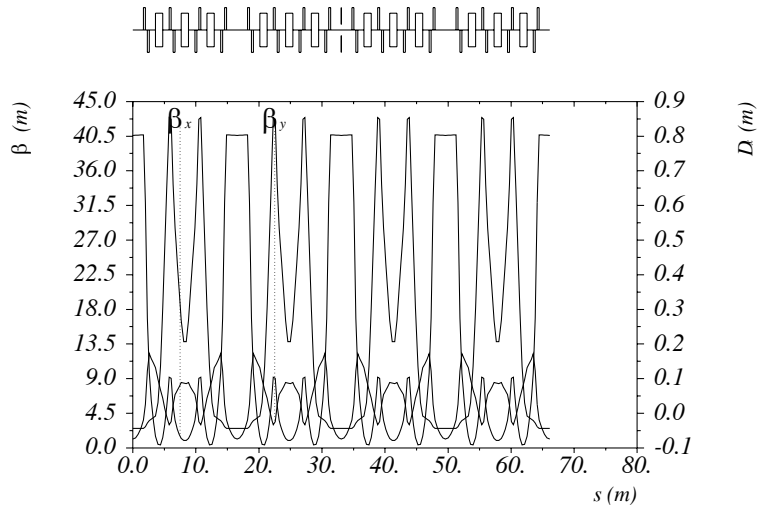

Fig. 1. The β functions and the dispersion function of HLS storage ring in HBLS mode.

2. Magnetic Field Model of the Wiggler

The wiggler that is installed in the HLS storage ring has single period composed of three poles, and the peak magnetic field strength of the central pole and the poles in either side is 6 T and 4.3 T respectively. The magnetic field of the wiggler is shown in Fig. 2, but we do not have the explicit data of the curve. Because of the lack of the wiggler field data, only the linear effects of it were studied by the hard edge model.[1,2] In the following we will build up an analytic magnetic field model similar enough to the real wiggler field, by which we can study both the linear effects and the nonlinear effects. And if our model wiggler can work on the HBLS mode, we can reasonably assume the real wiggler can also work in that mode.

A model of the wiggler's magnetic field can be generated by COSY Infinity 9.0.[3,4] Considering the motion of the electrons in the wiggler, we can reasonably assume the traces of the electrons are close to the axis of the wiggler, so that the electrons can not see the drop of the fringe field in x direction when the wiggler has enough width. Then the midplane field can be described by the following formulas.[3] The periodic field can be described as

$$B_m(x,z) = B_0 \cos\left(\frac{2\pi}{\lambda}\cdot z + k\cdot z^2\right), \tag{1}$$

in which λ is the wavelength of the wiggler, and the item $k\cdot z^2$ is used when the wiggler has a changing wavelength respect to z. The formula for the left fringe field is

$$B_l = K_l \cdot B_m(x,z), \tag{2}$$

$$\text{with } K_l = \frac{1}{1+\exp(a_0 + a_1(-z+z_l)/d + \cdots + a_9((-z+z_l)/d)^9)}. \tag{3}$$

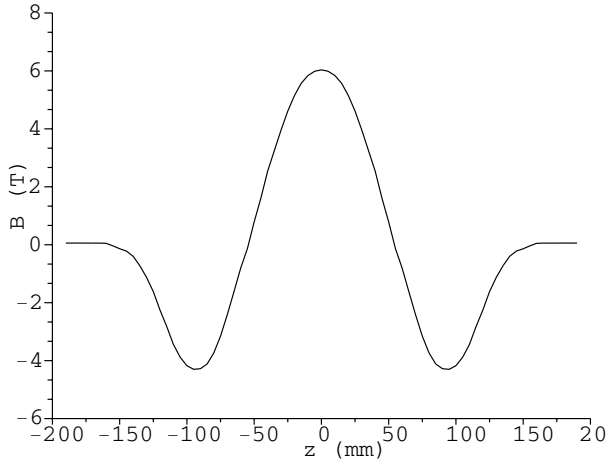

Fig. 2. The midplane magnetic fields of the wiggler.

When z goes to $-\infty$, $B_l(x,z)$ goes to 0, while when z goes to $+\infty$, $B_l(x,z)$ goes to $B_m(x,z)$. So we can get a good model of the fringe field by carefully customizing the coefficients $a_0, a_1, \ldots, a_9$, and d. In a similar way, the right fringe field can be described as

$$B_r = K_r \cdot B_m(x,z), \tag{4}$$

$$\text{with } K_r = \frac{1}{1+\exp(a_0 + a_1(z-z_r)/d + \cdots + a_9((z-z_r)/d)^9)}. \tag{5}$$

So that the whole magnetic field of wiggler can be described as

$$B = K_l \cdot B_m(x,z) \cdot K_r. \tag{6}$$

In our case, we choose $\lambda = 210$ mm, $k = 0$, $B_0 = 6.08$ T, $d = 40$ mm, $l = z_r - z_l = 252$ mm, $a_0 = 0.478959$, $a_1 = 1.911289$, $a_2, a_3, \ldots, a_{10} = 0$. The magnetic field of the model wiggler is shown in Fig. 3, comparing with the magnetic field of the real wiggler. We can see that we have arrived at a good model of the wiggler's magnetic field.

The 3D magnetic field can be generated in the following way.[5] Maxwell's equations of the magnetic field are

$$\overrightarrow{\nabla} \cdot \overrightarrow{D} = \rho, \overrightarrow{\nabla} \times \overrightarrow{E} = -\frac{\partial \overrightarrow{B}}{\partial t}. \tag{7}$$

If we only consider the field without time dependence in the region where there are no sources of the field, Maxwell's equations can be simplified as

$$\overrightarrow{\nabla} \cdot \overrightarrow{D} = 0, \overrightarrow{\nabla} \times \overrightarrow{E} = \overrightarrow{0}. \tag{8}$$

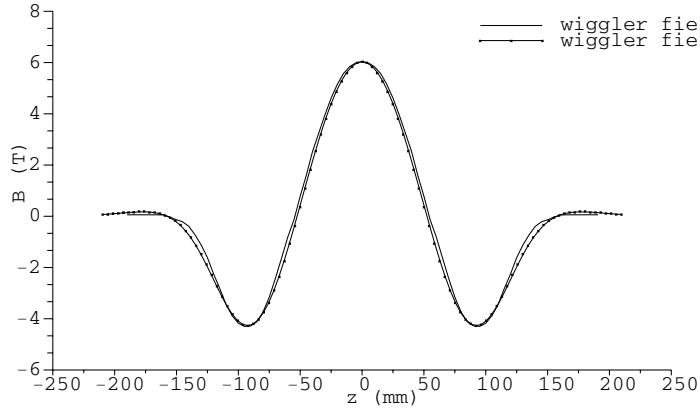

Fig. 3. The midplane magnetic field model of the wiggler.

In this case, $\overrightarrow{B}$ has a scalar potential V, which satisfies the Laplace equation

$$\triangle V = \frac{\partial^2 V}{\partial x^2} + \frac{\partial^2 V}{\partial y^2} + \frac{\partial^2 V}{\partial z^2} = 0, \tag{9}$$

and $\overrightarrow{B} = -\overrightarrow{\nabla} V$. The Eq. (9) can be rewritten in the fixed-point form as

$$V = O(V) = V|_{y=0} + \int_y \left\{ \frac{\partial}{\partial y} V|_{y=0} - \int_y \left(\frac{\partial}{\partial x} \left(\frac{\partial V}{\partial x} \right) + \frac{\partial}{\partial z} \left(\frac{\partial V}{\partial z} \right) \right) \right\} \tag{10}$$

The operator $O(V)$ on ${}_nD_3$ is contracting. And in the differential algebra (DA) picture, Eq. (10) can be easily solved to order n by iteratively applying the operator $O(V)$ on V for at most $n+1$ times, assuming V and $\partial V/\partial y$ are given in the $y = 0$ plane.

In the case of the wiggler, $\partial V/\partial y$ in the $y = 0$ plane is known as the midplane field. As the Eq. (6) shows, the midplane field does not explicitly depend on y, so the potential V in the $y = 0$ plane is simply $y \cdot \partial V/\partial y$. Solving the Eq. (10), we get the potential V, then the field at any point is just the gradient of the potential at the point. COSY Infinity 9.0 can calculate the field of the wiggler automatically.

3. Beam Dynamics Study by COSY Infinity 9.0

The tracking study of the beam dynamic effects of the wiggler was done by the COSY Infinity 9.0 beam physics package, which is based on DA arithmetic. After a storage ring was defined by the user, COSY can calculate the map of each element to arbitrary order, compose all the maps into a one-turn map of the storage ring, find the generating function of the one-turn map, then do the symplectic tracking by various methods.[3,5]

When the field of an element, such as a dipole, a quadruple, or a wiggler etc, is known, it is easy to write the dynamic equations of the electron motion as a group of ODE in the following form,

$$\dot{\vec{z}} = \vec{f}(\vec{z}, t), \tag{11}$$

where $\vec{z}$ is usually a 4D or 6D vector of positions and momenta. COSY has two methods to generate the map to arbitrary order from an given ODE.[5] One method is based on the antiderivation operator. Eq. (11) can be rewritten as

$$\vec{z} = O(\vec{z}) = \vec{z}_i + \int_{t_i}^{t} \vec{f}(\vec{z}, t')dt'. \tag{12}$$

The operator $O(\vec{z})$ on ${}_nD_v$ is contracting, and now we have a fixed-point problem again, which can be easily solved to the order n in the DA picture by iteratively acting the operator $O(\vec{z})$ at most $n+1$ times as we mentioned before. The integral in Eq. (12) can be done by the antiderivation operator in the DA picture. The other method is based on the derivation operator. For a given function $g(\vec{z}, t)$ in phase space, we have

$$\frac{d}{dt}g(\vec{z}, t) = \vec{f} \cdot \vec{\nabla} g + \frac{\partial}{\partial t} g = L_{\vec{f}} g, \tag{13}$$

where $L_{\vec{f}}$ is called Lie derivation operator, and $\dot{\vec{z}} = \vec{f}$ is the ODE we want to solve. The Taylor expansion of the solution of the ODE is

$$\vec{z}_f = \sum_{i=0}^{\infty} \frac{t^i \cdot L_{\vec{f}}^i}{i!} \cdot \vec{I}, \tag{14}$$

where $\vec{I}$ is the identity function. When g and $\vec{f}$ are not explicitly time dependant, the partial derivative respect to t in $L_{\vec{f}}$ disappear. If $\vec{f}(\vec{0}) = \vec{0}$, and letting g be a component of $\vec{z}$, we obtain the map

$$\vec{z}_0 = \vec{z}_i, \quad \vec{z}_j = \frac{t \cdot (\vec{f} \cdot \vec{\nabla})}{i} \cdot \vec{z}_{j-1}, \quad \vec{z}_f = \sum_{j=0}^{\infty} z_j. \tag{15}$$

As to the elements like dipoles, quadrupoles and etc, whose fields do not depend on the time variable, the derivation method works well. While the map of the elements like wigglers and undulators, whose fields change with the time variable, should be calculated by the antiderivation method.

The map of an element or a whole ring generated by COSY is described by an n-th order DA polynomial, so it is not symplectic because of the truncation. Symplectic Tracking is achieved in COSY by using the generating function, which can be easily calculated from a given map by DA method.[5] COSY provides the four basic types of generating functions[6] and the extended Poincare (EXPO) generating function, which in general gives optimal results in the weakly nonlinear case.[7,8] In the following, we will take the second kind of generating function as an example to

show how COSY works on this. Assume an origin preserving map M, we can write it as $M = (M_1, M_2)$, where M_1 is the position part, and M_2 is the momentum part. In the same way, we can write the identity map $I = (I_1, I_2)$. Let

$$N_1 = (I_1, M_2), \tag{16}$$

then

$$(\vec{q}_i, \vec{p}_f) = N_1(\vec{q}_i, \vec{p}_i), \text{ and } (\vec{q}_i, \vec{p}_i) = N_1^{-1}(\vec{q}_i, \vec{p}_f). \tag{17}$$

Let

$$N_2 = (M_1, I_2), \tag{18}$$

then

$$(\vec{q}_f, \vec{p}_i) = N_2(\vec{q}_i, \vec{p}_i) = N_2 \circ N_1^{-1}(\vec{q}_i, \vec{p}_f) = G(\vec{q}_i, \vec{p}_f). \tag{19}$$

The second kind of generating function F_2 satisfies

$$(\vec{q}_f, \vec{p}_i) = (\vec{\nabla}_{\vec{p}_f} F_2, \vec{\nabla}_{\vec{q}_i} F_2). \tag{20}$$

Comparing Eq. (19) with Eq. (20), we can see that F_2 is just a potential for G, which can be obtained by integration along an arbitrary path. The symplectic tracking can be performed in the following way. Firstly $\vec{p}_f$ can be solved from $\vec{p}_i = G_2(\vec{q}_i, \vec{p}_f)$ by some numerical method such as Newton iteration, where G_2 is the momentum part of Eq. (20). Then $\vec{q}_f$ can be calculated directly from $\vec{q}_f = G_1(\vec{q}_i, \vec{p}_f)$, where G_1 is the position part of Eq. (20).

In the above calculation of the generating function, the inverse map of N_1 needs to be calculated. This is also a fixed-point problem in DA picture, which can be easily solved.[5] Assuming A is a origin preserving map, it can be write as $A = A_1 + A_2$, where A_1 is the linear part of A, and A_2 is the nonlinear part of A. Then

$$A \circ A^{-1} = (A_1 + A_2) \circ A^{-1} = I \tag{21}$$

$$A^{-1} = O(A^{-1}) = A_1^{-1} \circ (I - A_2 \circ A^{-1}). \tag{22}$$

The Eq. (22) now has the fixed-point form and A_1^{-1} can be easily calculated since the Jacobian of the linear map A_1 is just a square matrix.

4. Linear Effects of the Wiggler

With the above model of the wiggler's magnetic field, we can calculate both the linear and the nonlinear map of it by COSY Infinity 9.0. The linear map of the wiggler is found to be

$$M_x = \begin{pmatrix} 0.9997516 & 0.2532518 \\ 0 & 1.000248 \end{pmatrix}, \; M_y = \begin{pmatrix} 0.9409307 & 0.2462244 \\ -0.4852251 & 0.9358029 \end{pmatrix}. \tag{23}$$

Under the effects of the wiggler, the tunes change from (5.2073,2.5351) into (5.2072, 2.5674). The horizontal tune almost remains the same value, while the vertical tune increases a little bit. This result is reasonable because the horizontal map is very similar to a drift map, but the vertical map shows the focusing effect of the wiggler. The positions of the tunes and the 3rd, 4th, 5th, and 6th order resonance lines nearby are shown in Fig. 4. Fortunately one observes that the position change of the tunes does not cross any third order resonance lines, because the third order resonance is dangerous and the beam will get lost if the resonance is strong enough.

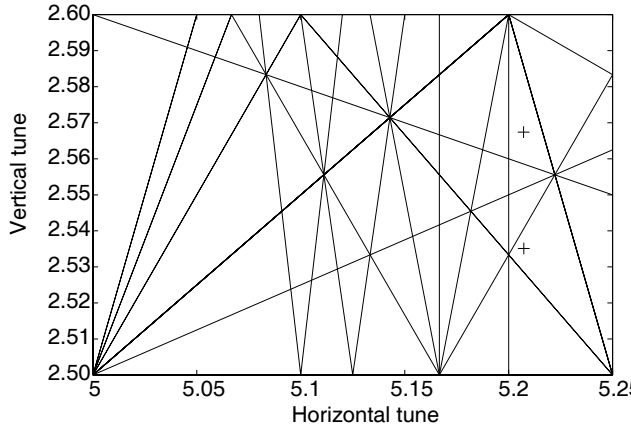

Fig. 4. The position change of the tunes and the 3rd, 4th, 5th, and 6th order resonance lines nearby.

The β functions with the wiggler are shown in Fig. 5. Comparing with Fig. 1, we can see the vertical β function is heavily disturbed, and the highest value increases from 11 m to 23 m. The changes of the vertical β functions are shown in Fig. 6. The increase of vertical β function will enlarge the close orbit distortion. It will also decrease the physical acceptance of the storage ring, and result in the decrease of the beam lifetime. So it is important to compensate the change of the β functions, and keep the tunes in a proper position at the same time. Generally it can be done by changing the strength of the quadrupoles in the storage ring, or adding extra quadrupoles on it.[1]

5. Effects of the Wiggler on Dynamic Apertures

To study the nonlinear effects of the wiggler, we concentrate on the change of the dynamic apertures with and without the wiggler. For each case, the one-turn map up to the 10th order was generated, and then the EXPO generating function was calculated from the map and was used for the symplectic tracking up to 5000 turns by COSY Infinity 9.0. The tunes were compensated back to the original values by

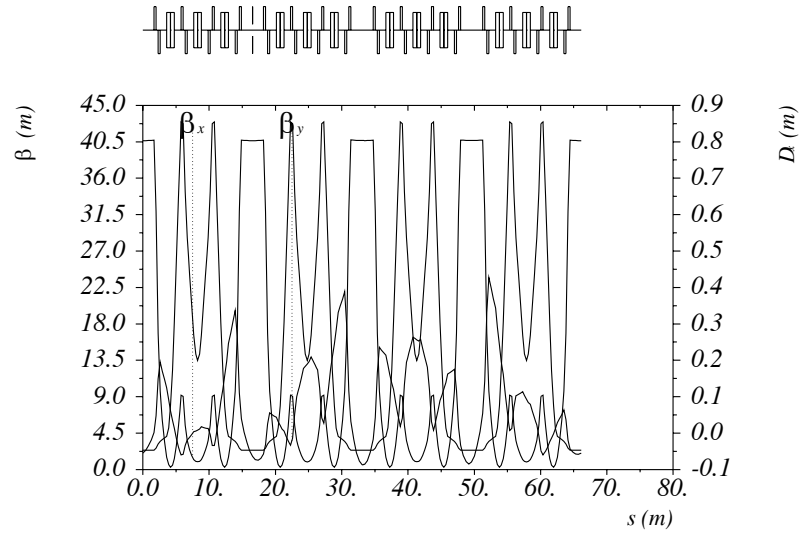

Fig. 5. The β functions and the dispersion function of HLS storage ring in HBLS mode with wiggler.

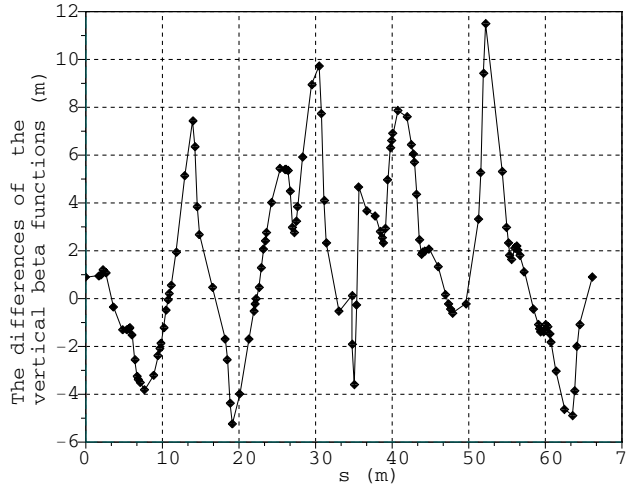

Fig. 6. The difference of the vertical β functions of HLS storage ring in HBLS mode with and without wiggler.

appropriately adjusting the strength of the quadrupoles before the tracking study in the case in which the wiggler is present, in order to avoid the change of the dynamic apertures due to the change of the global tunes. The tracking results of on-energy

particles in both x and y axis in bare lattice without the wiggler are shown in Fig. 7. The same tracking are made with the wiggler, and the results are shown in Fig. 8. In order to access the effects of the fringe field, we also trace the particles without the fringe field. In this case, the wiggler was treated as a periodic cosine magnetic field. The results are shown in Fig. 9. The traces in $x - a$ phase plane are almost the same. The dynamic aperture in horizontal direction is up to 26 mm.

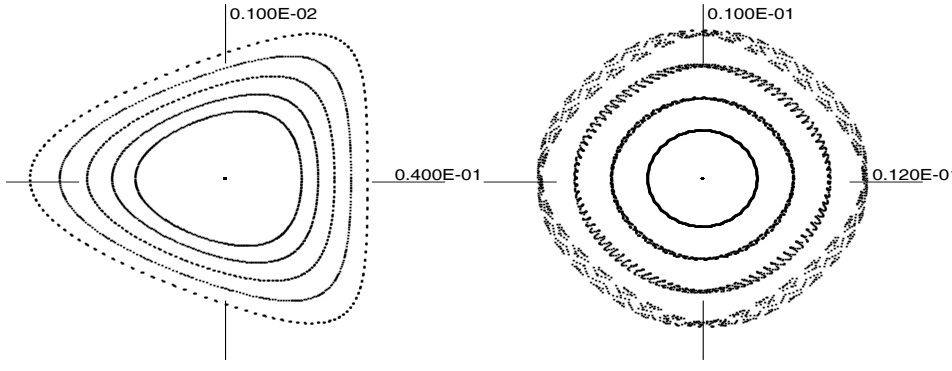

Fig. 7. Tracking pictures of on-energy particles launched along x axis and y axis without the wiggler.

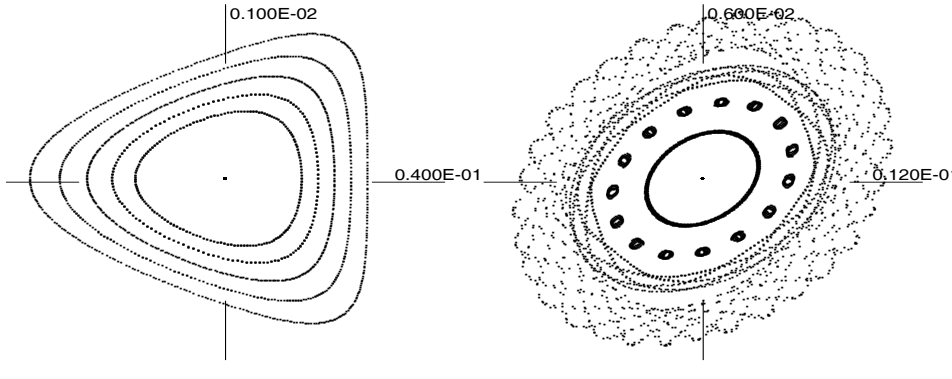

Fig. 8. Tracking pictures of on-energy particles launched along x axis and y axis with the wiggler.

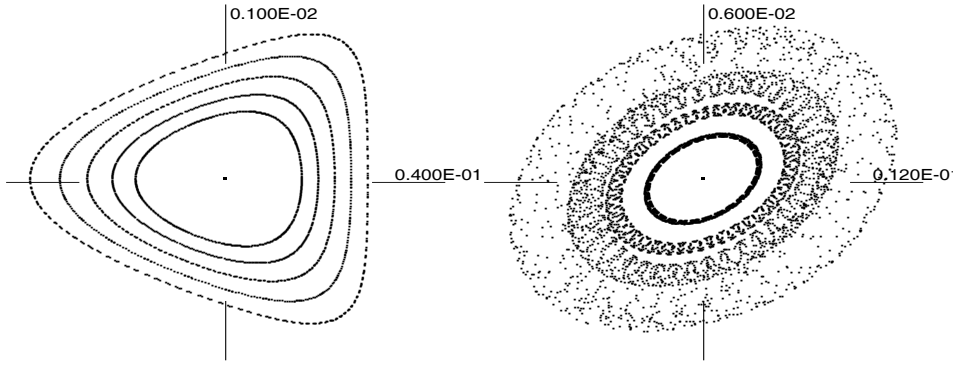

Fig. 9. Tracking pictures of on-energy particles launched along x axis and y axis with the wiggler but without considering the fringe field.

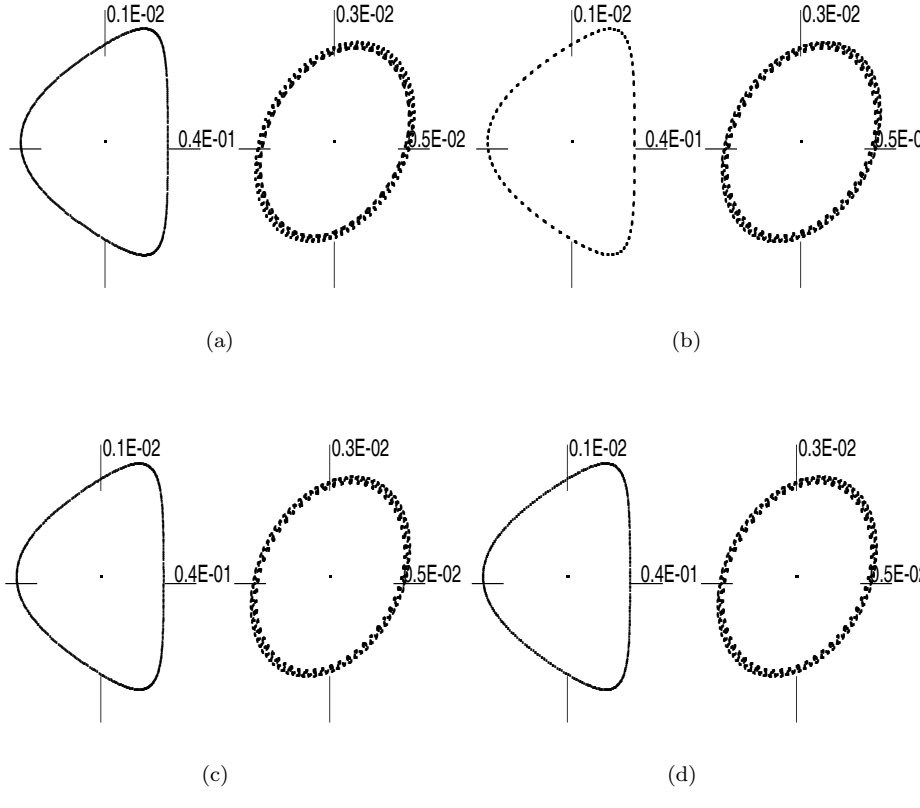

Fig. 10. Tracking pictures of on-energy particles launched at $x = 0.026$m, $y = 0$m (left) and $x = 0$m,$y = 0.004$m (right) with the wiggler up to the (a) 8th, (b) 9th, (c) 10th, (d) 11th order.

The traces in $y - b$ phase plane are different. Without the wiggler, the vertical dynamic aperture reaches 9 mm. With the wiggler, the particles might get lost at the island area in Fig. 8, which means the dynamic aperture decreases to about 4 mm. But it is still about 50 times of the vertical beam size at the middle point in the straight section, where the vertical beta function is only 2.03 m and the vertical beam size is only 0.07 mm.[9] In order to verify the dynamic apertures, we provide tracking pictures of the on-energy particles at $x = 0.026$ m, $y = 0$ m and $x = 0$ m, $y = 0.004$ m, with the EXPO generating functions of the 8th to the 11th order maps, which are shown in Fig. 10. And we can see these pictures agree with each other.

6. Conclusion

Considering the above results, we can draw the conclusion that the nonlinear affects of the wiggler will not seriously affect the performance of the storage ring, since the dynamic apertures with the wiggler are still large enough. But the vertical β function is distorted heavily because of the linear effects of the wiggler, which will decrease the physical acceptance and beam lifetime of the storage ring. The linear effects can be compensated by appropriately adjusting the strength of the quadruples. More work on the compensation should be done in the future.

References

1. L. Wang, H. Xu, G. Feng, and et al., Linear optics compensation of the superconducting wiggler in HLS, in *Proc. 2005 Particle Accelerator Conf.*, eds. B.Siemann (Knoxville, Tennessee, USA, 2005), p. 3037.
2. N. Liu, Y. Jin, H. Yan, and et al., Beam dynamic effects of 6 T superconducting wiggler on the Hefei light source storage ring, in *Development report of 6 T superconducting wiggler in NSRL*, (1999).
3. M. Berz, and K. Makino, COSY Infinity 9.0 beam physics manual, (2006), p. 17.
4. http://www.bt.pa.msu.edu/index_cosy.htm.
5. M. Berz, *Modern Map Methods in Particle Beam Physics*, 1st edn. (Academic Press, London, 1999).
6. H. Goldstein, C. Poole, and J. Safko, *Classical Mechanics*, 3rd edn. (Higher Education Press, Beijing, 2005), p. 373.
7. B. Erdelyi and and M. Berz, *Physical Review Letters* **87**, 11 (2001).
8. M.L. Shashikant, M. Berz, and B. Erdelyi, *Institute of Physics CS* **175** (2004).
9. H. Zhang, Study on the HLS high brilliance operation mode, Ph.D thesis, University of science and technology of China, (2006), p. 47.